

# Bipartite lattice of domain wall junction states in photonic lattices



Esteban F. Gutiérrez<sup>1\*</sup>, Francisco Muñoz<sup>2,3</sup>, Rodrigo A. Vicencio<sup>1</sup>.

<sup>1</sup> Departamento de Física and Millenium Institute for Research in Optics–MIRO, Facultad de Ciencias Físicas y Matemáticas, Universidad de Chile, 8370448 Santiago, Chile

<sup>2</sup> Departamento de Física, Facultad de Ciencias, Universidad de Chile, 9170124 Santiago, Chile

<sup>3</sup> Center for the Development of Nanoscience and Nanotechnology (CEDENNA), 9170124 Santiago, Chile

esteban.flores@ug.uchile.cl



## Introduction

The similarities between the Schrödinger equation in quantum mechanics and the paraxial wave equation in optics have allowed scientists to study quantum phenomena in photonic lattices [1,2]. The possibility of imaging the wave function directly using a CCD camera has emerged as a key advantage in optics in comparison to electronics systems [3].

This work suggests the observation of localized states of topological origin in waveguide arrays. In particular, we use a generalized Su-Schrieffer-Heeger (SSH) model [4,5].

## SSH and Domain-wall defect

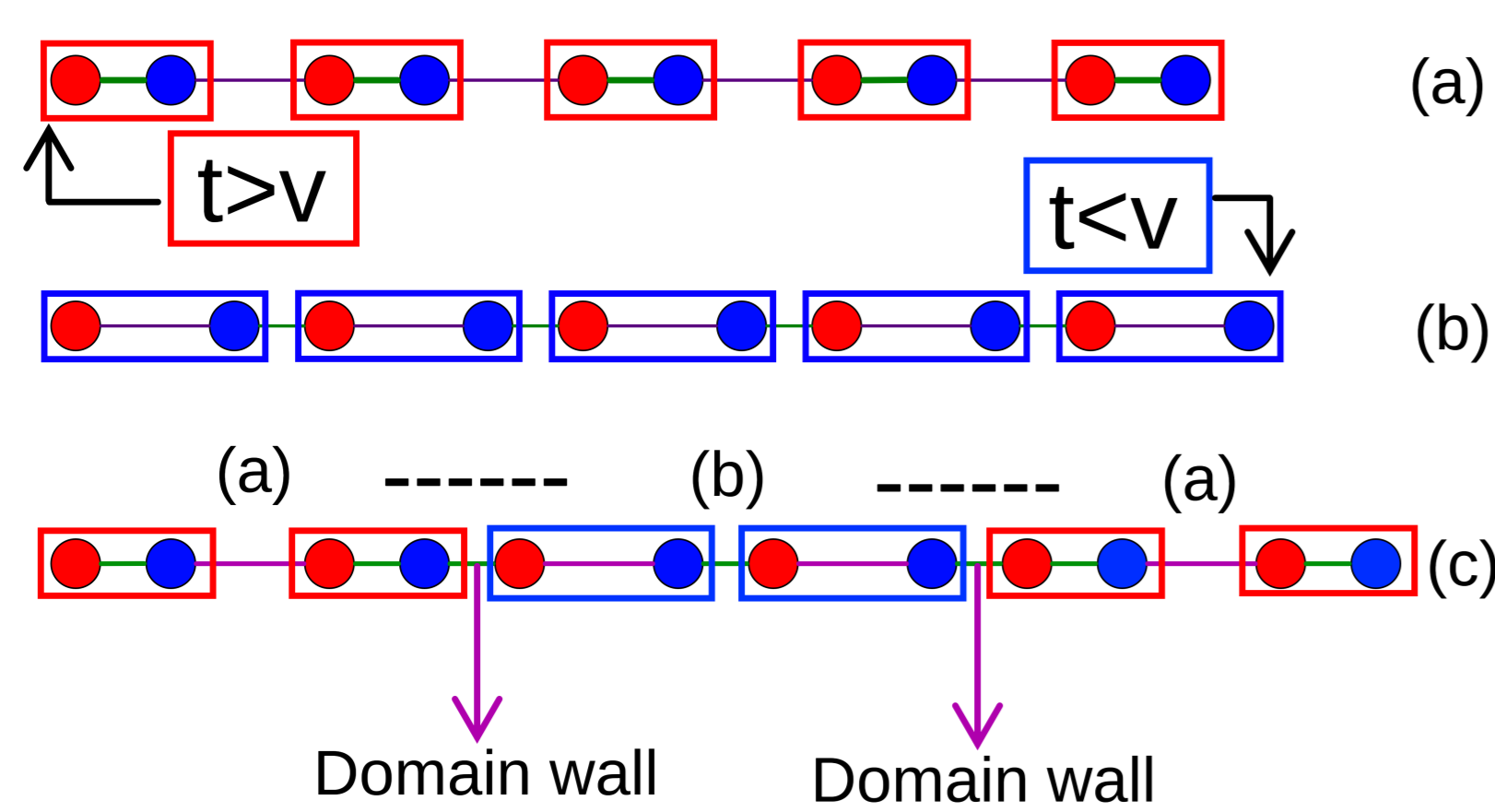


**Figure 1:** (a) Is a SSH chain with  $t > v$ , this is called as trivial case. (b) The topological case with intercell coupling greater than intracell constant, this is the topological case. Finally, (c) shows domain wall defects.

The primitive cell of SSH model is composed of two sites interacting between an intracell ( $t$ ) and an intercell ( $v$ ) coupling constant. The hopping ratio defines the topology of edge wavefunctions from a trivial insulator to a topological insulator.

The junction of two chains with different topology is known as a domain wall defect. In this geometry, a zero-energy localized state appear at the joint.

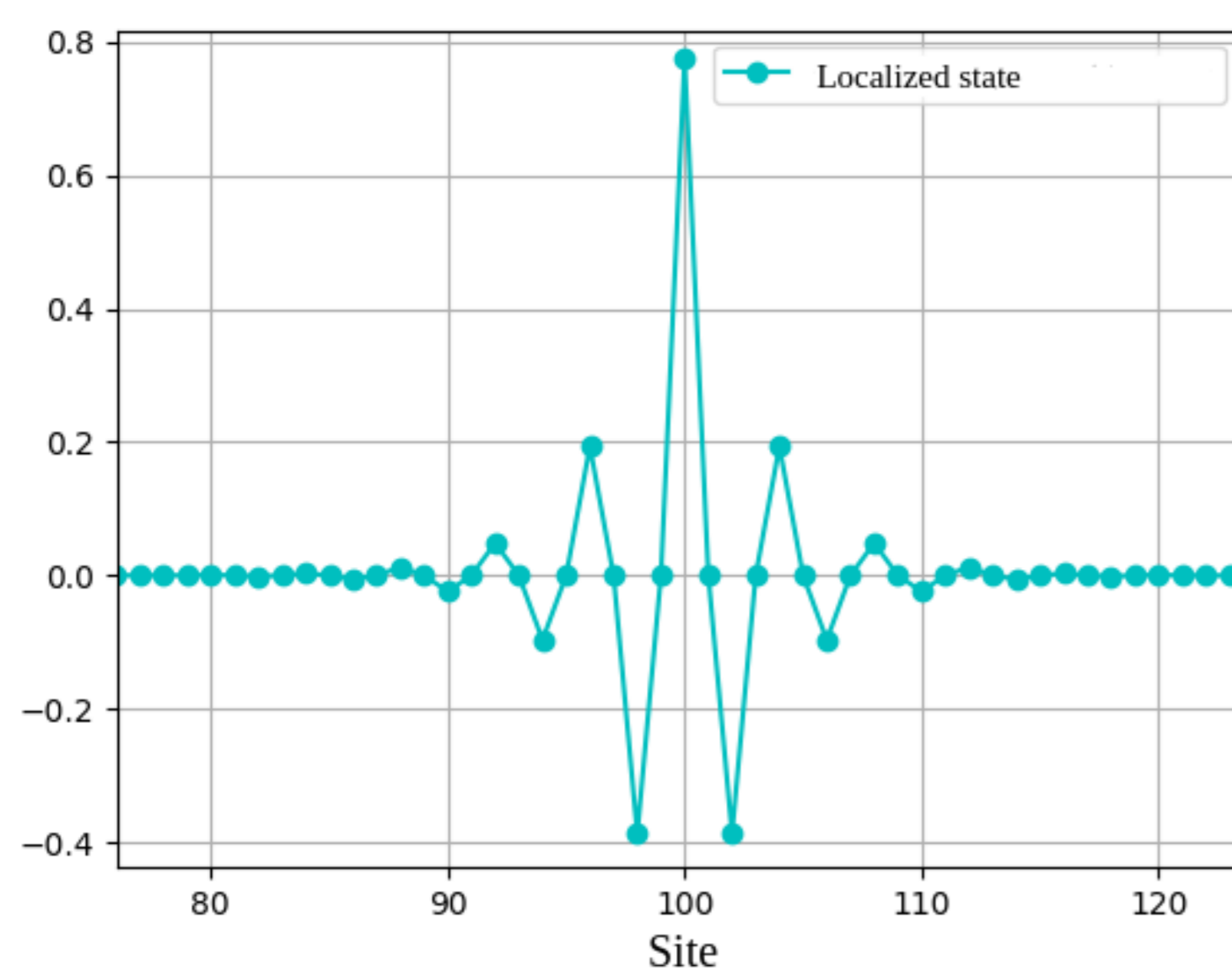
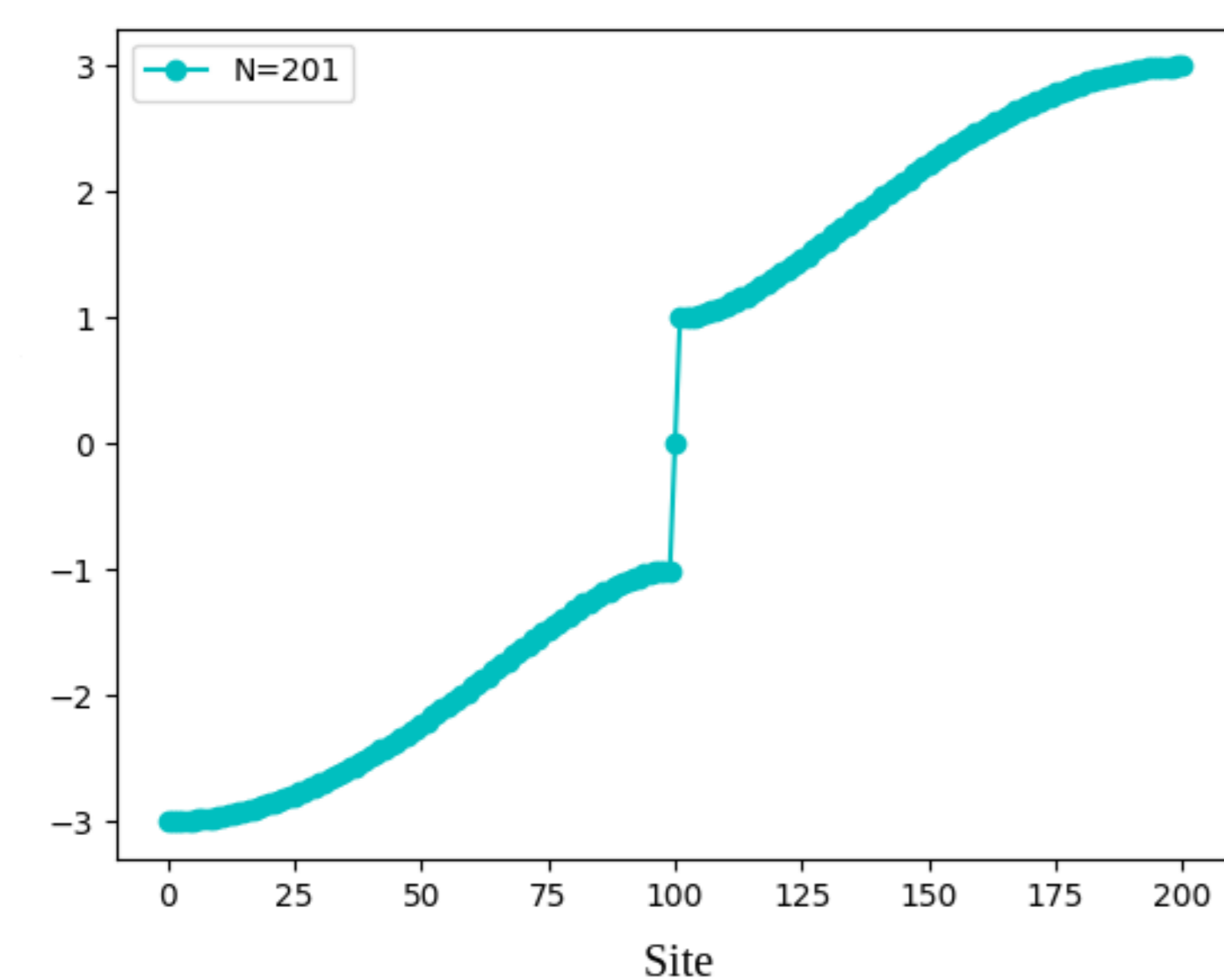


**Figure 2:** The upper shows the eigenvalues of the domain wall defect chain. In the lower it can be visualized the localized state in the center (junction) associated to the zero-energy state in the middle of the band.

Now, fixing the coupling constants, chains with different topology are concatenated by the following Hamiltonian (in second quantization):

$$H_{BDW} = \sum_{m=0}^{M+1} h_N(m) + \sum_{m=0}^M h'_{N'}(m)$$

$$h_N(m) = \sum_{j=m(N+N')}^{(m+1)N+mN'-1} (ta_j^\dagger b_j + va_{j+1}^\dagger b_j) + H.C \quad (1)$$

$$h'_{N'}(m) = \sum_{j=(m+1)N+(m+1)N'-1}^{(m+1)N+mN'} (va_j^\dagger b_j + ta_{j+1}^\dagger b_j) + H.C$$

where  $N$  and  $N'$  are the number of sites of the topological and trivial chain, respectively;  $M$  is the number of repetitions of domain wall defects and the total of sites in the geometry are  $c = M(N + N') + N$ . The main purpose of this, is to control the topology of the superlattice with the length not with the intercoupling and intracoupling constants.

Is important to note that the sum of  $h_N$  have an extra term. This is because the chain must be closed with the same chain with which it was started.

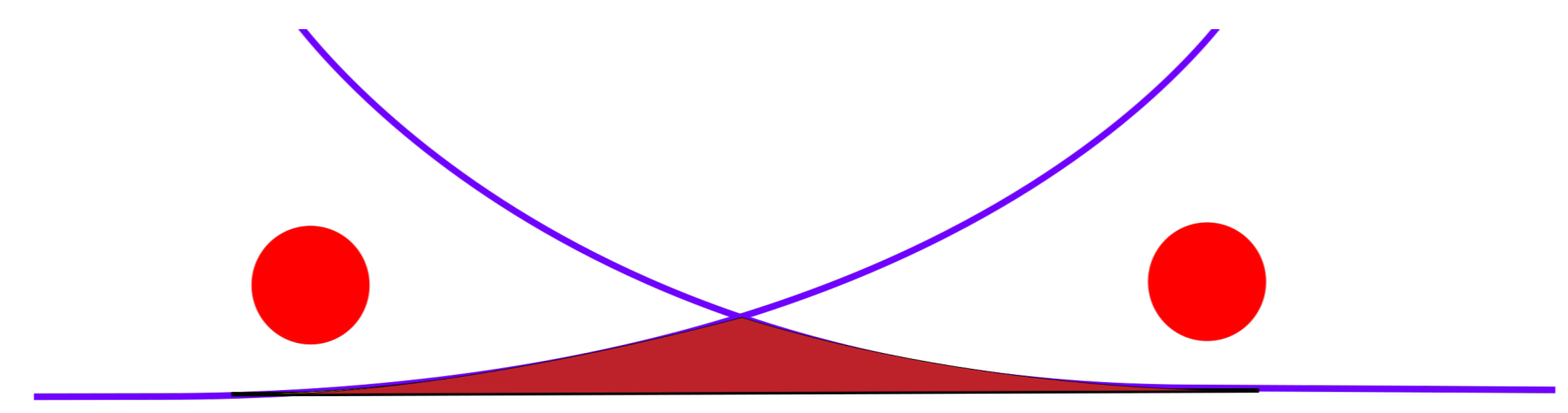


**Figure 3:** Junction states hybridize and interact between them with energy  $E_n = \pm t_n = \langle L|H|R \rangle \propto \exp-(n-1)$ .

## Results

All the results were obtained by numerical simulations solving the Hamiltonian and the DNLS equation. Firstly we use the results of the phase diagram in [5] to see how to obtain topological, trivial insulator or metallic phase.

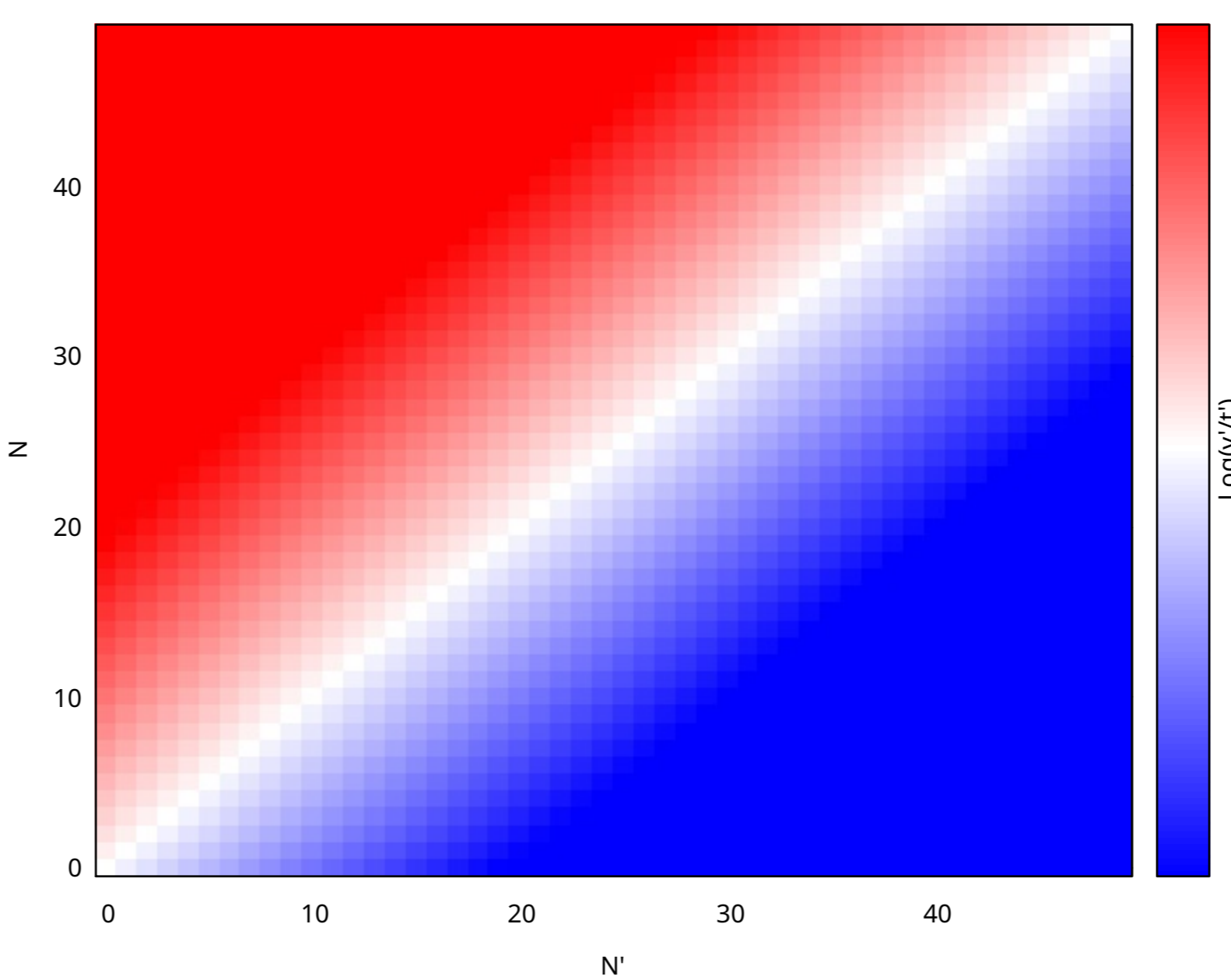


**Figure 4:** Phase diagram of winding number. The red zone is topological insulator, blue area is the trivial section and the central white is the metallic phase.

To see the transition and the emergence of the edge states, different output had been plotted in a heatmap diagram.

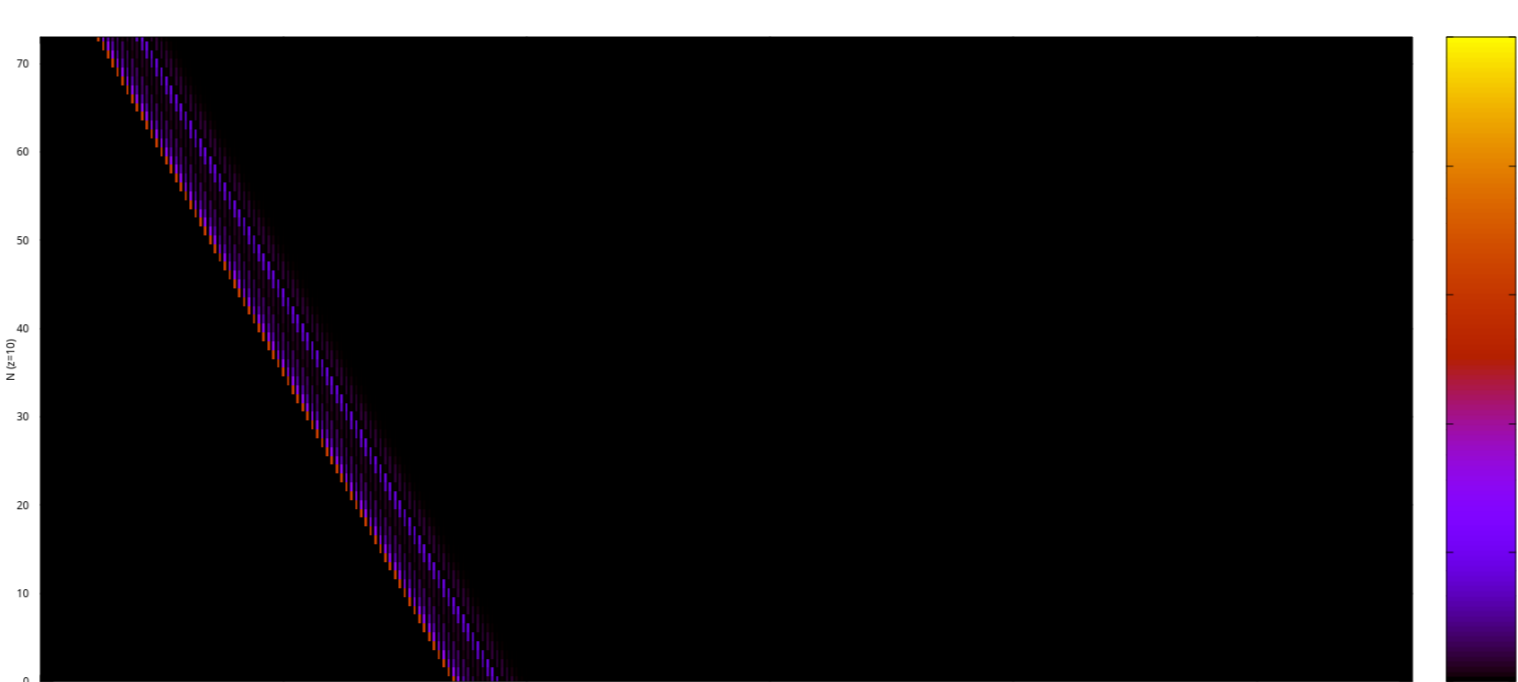


**Figure 5:** Output for different values of  $N = [6, 80]$ , a fixed value  $N' = 40$  and  $M = 4$ . In all of  $N$  have a edge states.

In the original SSH model [3], edge states only appear when the intercoupling amplitude is greater than intracoupling (only in the topological case), but now we have these

states for all values of  $N$ , even when is trivial ( $N < N'$ ). To understand this behaviour, the eigenstates with them eigenvalues has been obtained by solving (1) and using the Participation ratio  $R$  to see where are the localized states:

$$R = \frac{(\sum_i |\psi_i|^2)^2}{N (\sum_i |\psi_i|^4)}, \quad (2)$$

## Localized states

Focusing only on the near-zero-energy area, we observe that there exist  $2M + 2$  states, for the topological and trivial situation. In the first case, we use  $N = 16$ ,  $N' = 8$ ,  $M = 4$  and we observe two zero-energy states, and that, precisely are the localized edge states.

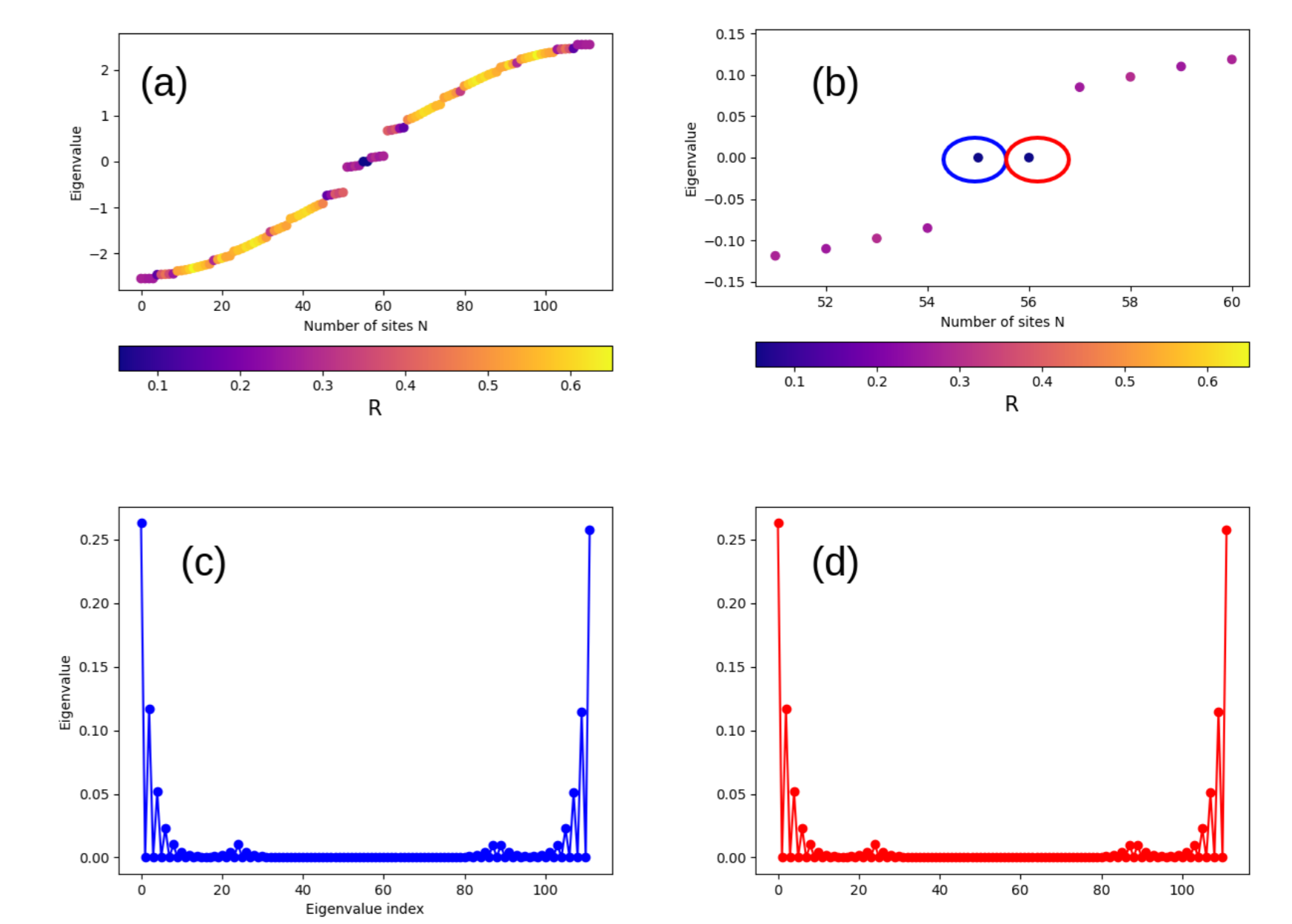


**Figure 6:** Near-zero-energy band for the topological situation. We observe localized states at the zero-energy.

For the trivial case, again we focus on the near-zero energy band. There are localized states in that zone, but is not in the Fermi energy, is in the extreme for lower and upper energies.

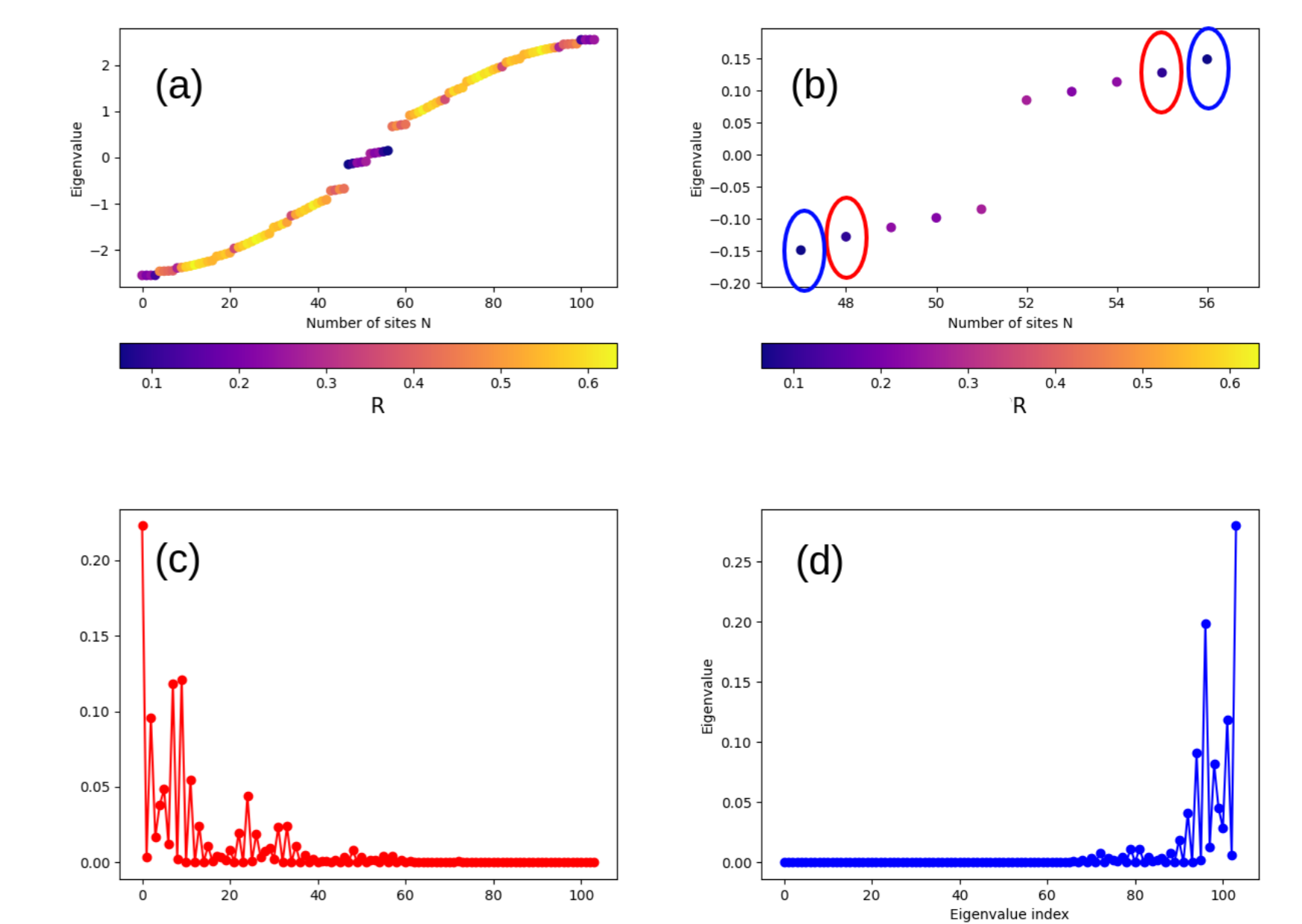


**Figure 7:** Near-zero-energy band for the topological situation. In this case there are not states in the zero-energy, but there are edge states in the extreme of the band.

## Acknowledgments

This poster was supported in part by Millennium Science Initiative Program ICN17-012 and FONDECYT Grants No. 1191205

## References

- [1] F. Lederer et al., Phys. Rep. 463, 1 (2008).
- [2] Malkova, N., Hromada, I., Wang, X., Bryant, G., Chen, Z., Opt. Lett. 34, 1633-1635 (2009).
- [3] Szameit, A., Nolte, S. J. Phys. B: At. Mol. Opt. Phys. 43 163001 (2010).
- [4] W. P. Su, J. R. Schrieffer, A. J. Heeger. Phys-RevLett.42.1698 (1979).
- [5] Muñoz, F., Pinilla, F., Mella, J., Molina, M. Sci Rep 8, 17330 (2018).